

3.3. TWINNING OF CRYSTALS

contrast, $6'(2)$ would designate a (polychromatic) twin axis which relates three domain states (three colours), each of *eigensymmetry* 2. Twin centres of symmetry $\bar{1}'$ are always added to the symbol in order to bring out an inversion twinning contained in the twin law. In the original version of Curien & Donnay (1959), the black–white symbols were only used for twinning by merohedry. In the present chapter, the symbols are also applied to non-merohedral twins, as is customary for (ferroelastic) domain structures. This has the consequence, however, that the *eigensymmetries* \mathcal{H} or \mathcal{H}' and the composite symmetries \mathcal{K} or \mathcal{K}' may belong to different crystal systems and, thus, are referred to different coordinate systems, as shown for the composite symmetry of gypsum in Section 3.3.4.1.

For the treatment of *multiple twins*, ‘polychromatic’ composite groups $\mathcal{K}(n)$ are required. These contain colour-changing operations of order higher than 2, *i.e.* they relate three or more colours (domain states). Consequently, not all pairs of domain states are transposable. This treatment of multiple twins is rather complicated and only sensible if the composite symmetry group is finite and contains twin axes of low order ($n \leq 8$). For this reason, the symbols for the composite symmetry \mathcal{K} of multiple twins are written without primes; see the examples in Section 3.3.4.4(iii).

3.3.6. Examples of twinned crystals

In order to illustrate the foregoing rather abstract deliberations, an extensive set of examples of twins occurring either in nature or in the laboratory is presented below. In each case, the twin law is described in two ways: by the coset of alternative twin operations and by the black–white symmetry symbol of the composite symmetry \mathcal{K} , as described in Sections 3.3.4 and 3.3.5.

For the description of a twin, the conventional crystallographic coordinate system of the crystal and its *eigensymmetry* group \mathcal{H} are used in general; exceptions are specifically stated. To indicate the orientation of the twin elements (both rational and irrational) and the composition planes, no specific convention has been adopted; rather a variety of intuitively understandable simple symbols are chosen for each particular case, with the additional remark ‘rational’ or ‘irrational’ where necessary. Thus, for twin reflection planes and (planar) twin boundaries symbols such as m_x , $m(100)$, $m \parallel (100)$ or $m \perp [100]$ are used, whereas twin rotation axes are designated by 2_z , $2_{[001]}$, $2 \parallel [001]$, $2 \perp (001)$, 3_z , $3_{[111]}$, $4_{[001]}$ *etc.*

3.3.6.1. Inversion twins in orthorhombic crystals

The (polar) 180° twin domains in a (potentially ferroelectric) crystal of *eigensymmetry* $\mathcal{H} = mm2$ ($m_x m_y 2_z$) and composite symmetry $\mathcal{K} = 2/m 2/m 2/m$ (*e.g.* in KTiOPO_4 , NH_4LiSO_4 , Li-formate monohydrate) result from a group–subgroup relation of index $[i] = 2$ with invariance of the symmetry framework (merohedral twins), but antiparallel orientation of the polar axes. The orientation relation between the two domain states is described by the coset $k \times \mathcal{H}$ of twin operations shown in Table 3.3.6.1, whereby the reflection in (001), m_z , is considered as the ‘representative’ twin operation.

Table 3.3.6.1. Orthorhombic inversion twins: coset of alternative twin operations (twin law)

\mathcal{H}	$k \times \mathcal{H} = m_z \times \mathcal{H}$
1	m_z (normal to the polar axis [001])
m_x	2_x (normal to the polar axis)
m_y	2_y (normal to the polar axis)
2_z	$\bar{1}$ (inversion)

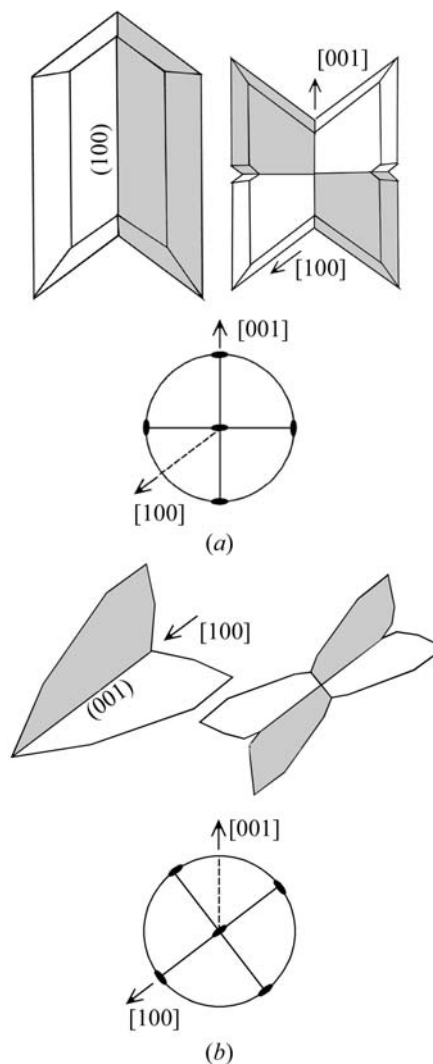


Fig. 3.3.6.1. Dovetail twin (a) and Montmartre twin (b) of gypsum. The two orientation states of each twin are distinguished by shading. For each twin type (a) and (b), the following aspects are given: (i) two idealized illustrations of each twin, on the left in the most frequent form with two twin components, on the right in the rare form with four twin components, the morphology of which displays the orthorhombic composite symmetry; (ii) the oriented composite symmetry in stereographic projection (dotted lines indicate monoclinic axes).

Hence, these twins can be regarded not only as reflection, but also as rotation or inversion twins. The composite symmetry, in black–white symmetry notation, is

$$\mathcal{K} = \frac{2'_x 2'_y 2'_z}{m_x m_y m'_z} (\bar{1}'),$$

whereby the primed symbols designate the (alternative) twin operations (*cf.* Section 3.3.5).

3.3.6.2. Twinning of gypsum

The *dovetail twin* of gypsum [*eigensymmetry* $\mathcal{H} = 1 2/m 1$, with twin reflection plane $m \parallel (100)$], coset of twin operations $k \times \mathcal{H}$ and composite symmetry \mathcal{K} , was treated in Section 3.3.4. Gypsum exhibits an independent additional kind of growth twinning, the *Montmartre twin* with twin reflection plane $m \parallel (001)$. These two twin laws are depicted in Fig. 3.3.6.1. The two cosets of twin operations in Table 3.3.6.2 and the symbols of the composite symmetries \mathcal{K}_D and \mathcal{K}_M of both twins are referred, in addition to the monoclinic crystal axes, also to orthorhombic axes x_D, y, z_D for dovetail twins and x_M, y, z_M for Montmartre twins. This procedure brings out for each case the perpendicularity of the

3. PHASE TRANSITIONS, TWINNING AND DOMAIN STRUCTURES

Table 3.3.6.2. Gypsum: cosets of alternative twin operations of the dovetail and the Montmartre twins, referred to their specific orthorhombic axes (subscripts D and M)

\mathcal{H}	Dovetail twins $m_{xD} \times \mathcal{H}$	Montmartre twins $m_{zM} \times \mathcal{H}$
1	$m_{xD} = m \parallel (100)$ (rational)	$m_{zM} = m \parallel (001)$ (rational)
$2_y = 2 \parallel [010]$	$m_{zD} = m \perp [001]$ (irrational)	$m_{xM} = m \perp [100]$ (irrational)
$m_y = m \parallel (010)$	$2_{zD} = 2 \parallel [001]$ (rational)	$2_{xM} = 2 \parallel [100]$ (rational)
$\bar{1}$	$2_{xD} = 2 \perp (100)$ (irrational)	$2_{zM} = 2 \perp [001]$ (irrational)

rational and irrational twin elements, clearly visible in Fig. 3.3.6.1, as follows:

$$\mathcal{K}_D = \frac{2'_{xD} \ 2_y \ 2'_{zD}}{m'_{xD} \ m_y \ m'_{zD}} \quad \mathcal{K}_M = \frac{2'_{xM} \ 2_y \ 2'_{zM}}{m'_{xM} \ m_y \ m'_{zM}}$$

$$x_D \text{ (ortho)} \perp (100) \text{ (mono)} \quad x_M \text{ (ortho)} \parallel [100] \text{ (mono)}$$

$$z_D \text{ (ortho)} \parallel [001] \text{ (mono)} \quad z_M \text{ (ortho)} \perp (001) \text{ (mono)}.$$

In both cases, the (*eigensymmetry*) framework $2_y/m_y$ is invariant under all twin operations; hence, the composite symmetries \mathcal{K}_D and \mathcal{K}_M are crystallographic of type $2/m2/m2/m$ (super-group index [2]) but differently oriented, as shown in Fig. 3.3.6.1. There is no physical reality behind the orthorhombic symmetry of the two \mathcal{K} groups: gypsum is neither structurally nor metrically pseudo-orthorhombic, the monoclinic angle being 128° . The two \mathcal{K} groups and their orthorhombic symbols, however, clearly reveal the two different twin symmetries and, for each case, the perpendicular orientations of the four twin elements, two rational and two irrational. The two twin types originate from independent nucleation in aqueous solutions.

It should be noted that for *all* (potential) twin reflection planes ($h0l$) in the zone $[010]$ (monoclinic axis), the oriented *eigensymmetry* $\mathcal{H} = 12/m1$ would be the same for all domain states, *i.e.* the intersection symmetry \mathcal{H}^* is identical with the oriented *eigensymmetry* \mathcal{H} and, thus, the composite symmetry would be always crystallographic.

For a more general twin reflection plane not belonging to the zone ($h0l$), such as (111), however, the oriented *eigensymmetry* \mathcal{H} would not be invariant under the twin operation. Consequently, an additional twin reflection plane ($\bar{1}\bar{1}\bar{1}$), equivalent with respect to the *eigensymmetry* $12/m1$, exists. This (hypothetical) twin would belong to category (ii) in Section 3.3.4.4 and would formally lead to a noncrystallographic composite symmetry of infinite order. If, however, we restrict our considerations to the intersection symmetry $\mathcal{H}^* = \bar{1}$ of a domain pair, the reduced composite symmetry $\mathcal{K}^* = 2'/m'$ with $m' \parallel (111)$ and $2' \perp (111)$ (irrational) would result. Note that for these (hypothetical) twins the reduced composite symmetry \mathcal{K}^* and the *eigensymmetry* \mathcal{H} are isomorphic groups, but that their orientations are quite different.

Remark. In the domain-structure approach, presented in Chapter 3.4 of this volume, both gypsum twins, dovetail and Montmartre, can be derived together as a result of a single (hypothetical) ferroelastic phase transition from a (nonexistent) orthorhombic parent phase of symmetry $\mathcal{G} = 2/m2/m2/m$ to a monoclinic daughter phase of symmetry $\mathcal{H} = 12/m1$, with a very strong metrical distortion of 38° from $\beta = 90^\circ$ to $\beta = 128^\circ$ (Janovec, 2003). In this (hypothetical) transition the two mirror planes, (100) and (001), 90° apart in the orthorhombic form, become twin reflection planes of monoclinic gypsum, (100) for the dovetail, (001) for the Montmartre twin law, with an angle of 128° . It must be realized, however, that neither the orthorhombic parent phase nor the ferroelastic phase transition are real.

3.3.6.3. Twinning of low-temperature quartz (α -quartz)

Quartz is a mineral which is particularly rich in twinning. It has the noncentrosymmetric trigonal point group 32 with three polar

twofold axes and a non-polar trigonal axis. The crystals exhibit enantiomorphism (right- and left-handed quartz), piezoelectricity and optical activity. The lattice of quartz is hexagonal with holohedral (lattice) point group $6/m2/m2/m$. Many types of twin laws have been found (*cf.* Frondel, 1962), but only the four most important ones are discussed here:

- Dauphiné twins;
- Brazil twins;
- Combined-law (Leydolt, Liebisch) twins;
- Japanese twins.

The first three types are merohedral (parallel-lattice) twins and their composite symmetries belong to category (i) in Section 3.3.4.2, whereas the non-merohedral Japanese twins (twins with inclined lattices or inclined axes) belong to category (ii).

3.3.6.3.1. Dauphiné twins

This twinning is commonly described by a twofold twin rotation around the threefold symmetry axis $[001]$. The two orientation states are of equal handedness but their polar axes are reversed ('electrical twins'). Dauphiné twins can be transformation or growth or mechanical (ferroelastic) twins. The composite symmetry is $\mathcal{K} = 622$, the point group of high-temperature quartz (β -quartz). The coset decomposition of \mathcal{K} with respect to the *eigensymmetry* $\mathcal{H} = 32$ (index [2]) contains the operations listed in Table 3.3.6.3.

The left coset $2_z \times \mathcal{H}$ constitutes the twin law. Note that this coset contains four twofold rotations of which the first one, 2_z , is the standard description of Dauphiné twinning. In addition, the coset contains two sixfold rotations, 6^1 and $6^5 = 6^{-1}$. The black-white symmetry symbol of the composite symmetry is $\mathcal{K} = 6'(3)22'$ (super-group of index [2] of the *eigensymmetry* group $\mathcal{H} = 32$).

This coset decomposition $622 \Rightarrow 32$ was first listed and applied to quartz by Janovec (1972, p. 993).

3.3.6.3.2. Brazil twins

This twinning is commonly described by a twin reflection across a plane normal to a twofold symmetry axis. The two orientation states are of opposite handedness (*i.e.* the sense of the optical activity is reversed: optical twins) and the polar axes are reversed as well. The coset representing the twin law consists of the following six operations:

(i) three reflections across planes $\{11\bar{2}0\}$, normal to the three twofold axes;

(ii) three rotoinversions $\bar{3}$ around $[001]$: $\bar{3}^1, \bar{3}^3 = \bar{1}, \bar{3}^5 = \bar{3}^{-1}$.

The coset shows that Brazil twins can equally well be described as reflection or inversion twins. The composite symmetry

Table 3.3.6.3. Dauphiné twins of α -quartz: coset of alternative twin operations (twin law)

\mathcal{H}	$2_z \times \mathcal{H}$
1	$2_z = 6^3$
3^1	$6^5 (= 6^{-1})$
3^2	6^1
$2_{[100]}$	$2_z \times 2_{[100]} = 2_{[120]}$
$2_{[010]}$	$2_z \times 2_{[010]} = 2_{[210]}$
$2_{[\bar{1}\bar{1}0]}$	$2_z \times 2_{[\bar{1}\bar{1}0]} = 2_{[\bar{1}\bar{1}0]}$

3.3. TWINNING OF CRYSTALS

$$\mathcal{K} = \bar{3}'(3) \frac{2}{m'} 1(\bar{1}')$$

is a supergroup of index [2] of the *eigensymmetry* group 32.

3.3.6.3.3. Combined Dauphiné–Brazil (Leydolt, Liebisch) twins

Twins of this type can be described by a twin reflection across the plane (0001), normal to the threefold axis [001]. The two orientation states of this twin are of opposite handedness (*i.e.* the optical activity is reversed, optical twin), but the polar axes are not reversed. The coset representing the twin law consists of the following six operations:

(i) three twin reflections across planes $\{10\bar{1}0\}$, parallel to the three twofold axes;

(ii) three rotoinversions $\bar{6}$ around [001]: $\bar{6}^1, \bar{6}^3 = m_z, \bar{6}^5 = \bar{6}^{-1}$.

The composite symmetry

$$\mathcal{K} = \bar{6}'(3)2m' = \frac{3}{m'} 2m'$$

is again a supergroup of index [2] of the *eigensymmetry* group 32. This twin law is usually described as a combination of the Dauphiné and Brazil twin laws, *i.e.* as the twofold Dauphiné twin rotation 2_z followed by the Brazil twin reflection $m(11\bar{2}0)$ or, alternatively, by the inversion $\bar{1}$. The product $2_z \times \bar{1} = m_z$ results in a particularly simple description of the combined law as a reflection twin on m_z .

Twin domains of the Leydolt type are very rarely intergrown in direct contact, *i.e.* with a common boundary. If, however, a quartz crystal contains inserts of Dauphiné and Brazil twins, the domains of these two types, even though not in contact, are related by the Leydolt law. In this sense, Leydolt twinning is rather common in low-temperature quartz. In contrast, GaPO₄, a quartz homeotype with the berlinite structure, frequently contains Leydolt twin domains in direct contact, *i.e.* with a common boundary (Engel *et al.*, 1989).

In conclusion, the three merohedral twin laws of α -quartz described above imply four domain states with different orientations of important physical properties. These relations are shown in Fig. 3.3.6.2 for electrical polarity, optical activity and the orientation of etch pits on (0001). It is noteworthy that these three twin laws are the only possible merohedral twins of quartz, and that all three are realized in nature. Combined, they lead to the composite symmetry $\mathcal{K} = 6/m 2/m 2/m$ ('complete twin': Curien & Donnay, 1959).

In the three twin laws (cosets) above, only odd powers of 6, $\bar{3}$ and $\bar{6}$ (rotations and rotoinversions) occur as twin operations, whereas the even powers are part of the *eigensymmetry* 32. Consequently, repetition of any odd-power twin operation restores the original orientation state, *i.e.* each of these operations has the nature of a 'binary' twin operation and leads to a pair of *transposable* orientation states.

3.3.6.3.4. Japanese twins (or La Gardette twins)

Among the quartz twins with 'inclined axes' ('inclined lattices'), the Japanese twins are the most frequent and important

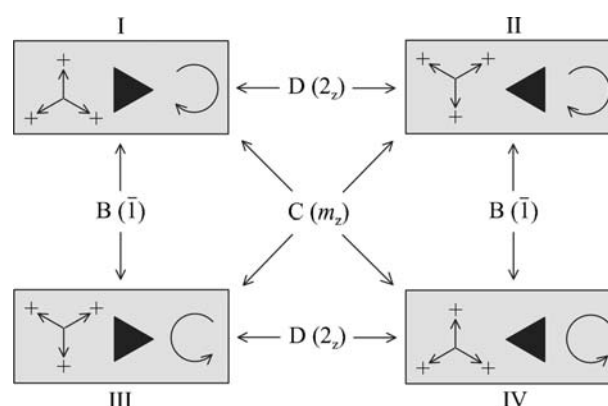


Fig. 3.3.6.2. Distinction of the four different domain states generated by the three merohedral twin laws of low-quartz and of quartz homeotypes such as GaPO₄ (Dauphiné, Brazil and Leydolt twins) by means of three properties: orientation of the three electrical axes (triangle of arrows), orientation of etch pits on (001) (solid triangle) and sense of the optical rotation (circular arrow). The twin laws relating two different domain states are indicated by arrows [D (2_z): Dauphiné law; B ($\bar{1}$): Brazil law; C (m_z): Leydolt law]. For GaPO₄, see Engel *et al.* (1989).

ones. They are contact twins of two individuals with composition plane (11 $\bar{2}$). This results in an angle of 84°33' between the two threefold axes. One pair of prism faces is parallel (coplanar) in both partners.

There exist four orientation relations, depending on

(i) the handedness of the two twin partners (equal or different);

(ii) the azimuthal difference (0 or 180°) around the threefold axis of the two partners.

These four variants are illustrated in Fig. 3.3.6.3 and listed in Table 3.3.6.4. The twin interface for all four twin laws is the same, (11 $\bar{2}$), but only in type III do twin mirror plane and composition plane coincide.

In all four types of Japanese twins, the intersection symmetry (reduced *eigensymmetry*) \mathcal{H}^* of a pair of twin partners is 1. Consequently, the twin laws (cosets) consist of only one twin operation and the reduced composite symmetry \mathcal{K}^* is a group of order 2, represented by the twin element listed in Table 3.3.6.4. If one were to use the full *eigensymmetry* $\mathcal{H} = 32$, the infinite sphere group would result as composite symmetry \mathcal{K} .

Many further quartz twins with inclined axes are described by Frondel (1962). A detailed study of these inclined-axis twins in terms of coincidence-site lattices (CSLs) is provided by McLaren (1986).

3.3.6.4. Twinning of high-temperature quartz (β -quartz)

Upon heating quartz into the hexagonal high-temperature phase (point group 622) above 846 K, the Dauphiné twinning disappears, because the composite symmetry \mathcal{K} of the twinned low-temperature phase now becomes the *eigensymmetry* \mathcal{H} of the high-temperature phase. For Brazil twins, however, their nature as reflection or inversion twins is preserved during the transformation.

Table 3.3.6.4. The four different variants of Japanese twins according to Frondel (1962)

Handedness of twin partners	Azimuthal difference (°)	Twin element = twin law	Label in Fig. 65 of Frondel (1962)
L–L or R–R	0	Irrational twofold twin axis normal to plane (11 $\bar{2}$)	I(R), I(L)
	180	Rational twofold twin axis $[11\bar{1}] \equiv [11\bar{2}]^\dagger$ parallel to plane (11 $\bar{2}$)	II(R), II(L)
L–R or R–L	0	Rational twin mirror plane (11 $\bar{2}$)	III
	180	Irrational twin mirror plane normal to direction $[11\bar{1}] \equiv [11\bar{2}]^\dagger$	IV

\dagger The line $[11\bar{1}] \equiv [11\bar{2}]$ is the edge between the faces $z(01\bar{1})$ and $r(10\bar{1}1)$ and is parallel to the composition plane (11 $\bar{2}$). It is parallel or normal to the four twin elements. Transformation formulae between the three-index and the four-index direction symbols, UVW and uvw , are given by Barrett & Massalski (1966, p. 13).

3. PHASE TRANSITIONS, TWINNING AND DOMAIN STRUCTURES

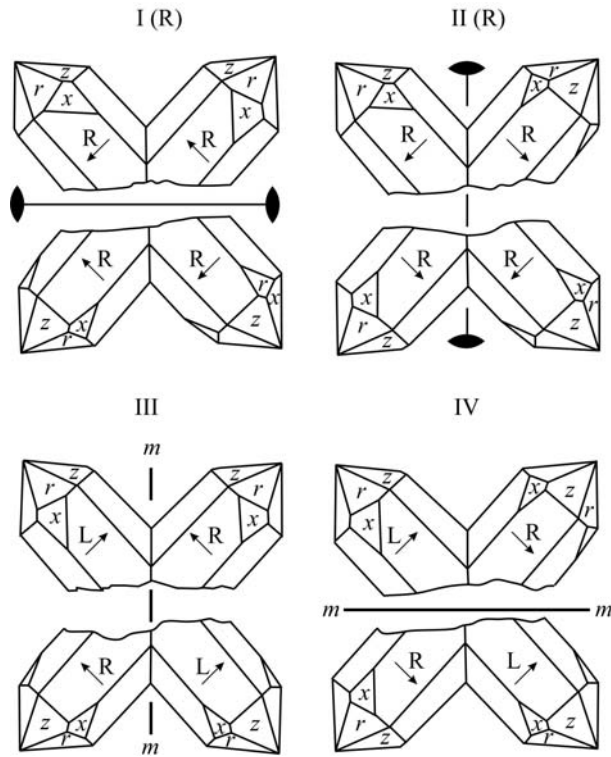


Fig. 3.3.6.3. The four variants of Japanese twins of quartz (after Frondel, 1962; cf. Heide, 1928). The twin elements 2 and m and their orientations are shown. In actual twins, only the upper part of each figure is realized. The lower part has been added for better understanding of the orientation relation. R, L: right-, left-handed quartz. The polarity of the twofold axis parallel to the plane of the drawing is indicated by an arrow. In addition to the cases I(R) and II(R), I(L) and II(L) also exist, but are not included in the figure. Note that a vertical line in the plane of the figure is the zone axis $[11\bar{1}]$ for the two rhombohedral faces r and z , and is parallel to the twin and composition plane ($11\bar{2}$) and the twin axis in variant II.

The *eigensymmetry* of high-temperature quartz is 622 (order 12). Hence, the coset of the Brazil twin law contains 12 twin operations, as follows:

- (i) the six twin operations of a Brazil twin in low-temperature quartz, as listed above in Example 3.3.6.3.2;
- (ii) three further reflections across planes $\{10\bar{1}0\}$, which bisect the three Brazil twin planes $\{11\bar{2}0\}$ of low-temperature quartz;
- (iii) three further rotoinversions around $[001]$: $\bar{6}^1$, $\bar{6}^3 = m_z$, $\bar{6}^5 = \bar{6}^{-1}$.

The composite symmetry is

$$\mathcal{K} = \frac{6}{m'} \frac{2}{m'} \frac{2}{m'} (\bar{1}'),$$

a supergroup of index [2] of the *eigensymmetry* 622 .

In high-temperature quartz, the combined Dauphiné–Brazil twins (Leydolt twins) are identical with Brazil twins, because the Dauphiné twin operation has become part of the *eigensymmetry* 622 . Accordingly, both kinds of twins of low-temperature quartz merge into one upon heating above 846 K. We recommend that these twins are called ‘Brazil twins’, independent of their type of twinning in the low-temperature phase. Upon cooling below 846 K, transformation Dauphiné twin domains may appear in both Brazil growth domains, leading to four orientation states as shown in Fig. 3.3.6.2. Among these four orientation states, two Leydolt pairs occur. Such Leydolt domains, however, are not necessarily in contact (cf. Example 3.3.6.3.3 above).

In addition to these twins with ‘parallel axes’ (merohedral twins), several kinds of growth twins with ‘inclined axes’ occur in high-temperature quartz. They are not treated here, but additional information is provided by Frondel (1962).

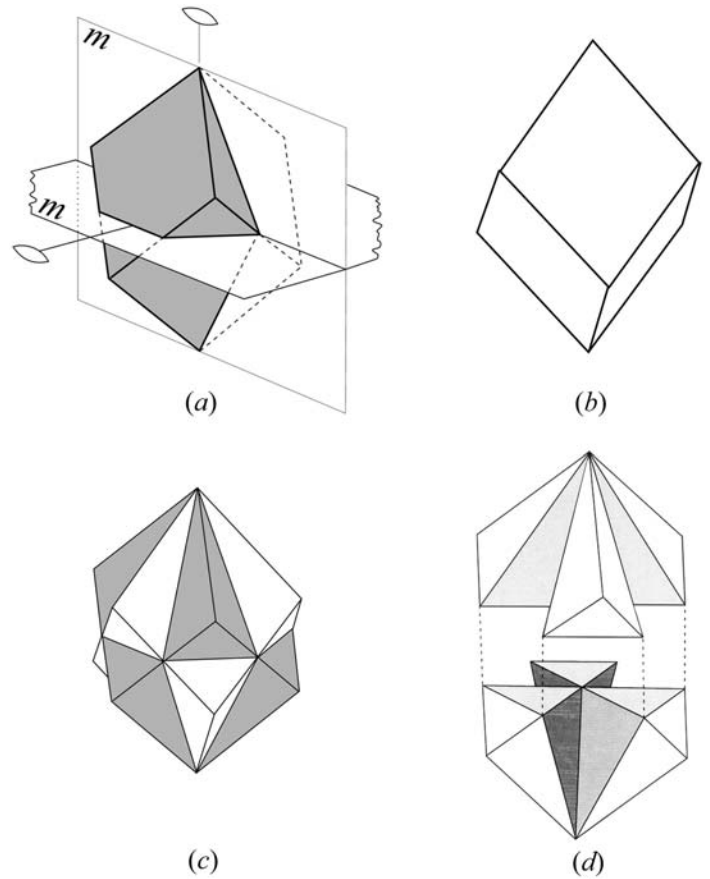


Fig. 3.3.6.4. Twin intergrowth of ‘obverse’ and ‘reverse’ rhombohedra of rhombohedral FeBO_3 . (a) ‘Obverse’ rhombohedron with four of the 12 alternative twin elements. (b) ‘Reverse’ rhombohedron (twin orientation). (c) Interpenetration of both rhombohedra, as observed in penetration twins of FeBO_3 . (d) Idealized skeleton of the six components (exploded along $[001]$ for better recognition) of the ‘obverse’ orientation state shown in (a). The components are connected at the edges along the threefold and the twofold eigensymmetry axes. The shaded faces are $\{10\bar{1}0\}$ and $\{0001\}$ coinciding twin reflection and contact planes with the twin components of the ‘reverse’ orientation state. Parts (a) to (c) courtesy of R. Diehl, Freiburg.

3.3.6.5. Twinning of rhombohedral crystals

In some rhombohedral crystals such as corundum Al_2O_3 (Wallace & White, 1967), calcite CaCO_3 or FeBO_3 (calcite structure) (Kotrbova *et al.*, 1985; Klapper, 1987), growth twinning with a ‘twofold twin rotation around the threefold symmetry axis $[001]$ ’ (similar to the Dauphiné twins in low-temperature quartz described above) is common. Owing to the *eigensymmetry* $\bar{3}2/m$ (order 12), the following 12 twin operations form the coset (twin law). They are described here in hexagonal axes:

- (i) three rotations around the threefold axis $[001]$: $\bar{6}^1$, $\bar{6}^3 = 2_z$, $\bar{6}^5 = \bar{6}^{-1}$;
- (ii) three twofold rotations around the axes $[120]$, $[210]$, $[\bar{1}\bar{1}0]$;
- (iii) three reflections across the planes $(10\bar{1}0)$, $(1\bar{1}00)$, $(01\bar{1}0)$;
- (iv) three rotoinversions around the threefold axis $[001]$: $\bar{6}^1$, $\bar{6}^3 = m_z$ and $\bar{6}^5 = \bar{6}^{-1}$.

Some of these twin elements are shown in Fig. 3.3.6.4. They include the particularly conspicuous twin reflection plane m_z perpendicular to the threefold axis $[001]$. The composite symmetry is

$$\mathcal{K} = \frac{6'}{m'} (\bar{3}) \frac{2}{m} \frac{2'}{m'} \quad (\text{order } 24).$$

It is of interest that for FeBO_3 crystals this twin law always, without exception, forms penetration twins (Fig. 3.3.6.4), whereas for the isotypic calcite CaCO_3 only $\{0001\}$ contact twins are found (Fig. 3.3.6.5). This aspect is discussed further in Section 3.3.8.6.

3.3. TWINNING OF CRYSTALS

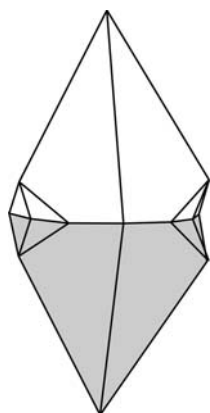


Fig. 3.3.6.5. Contact growth twin of calcite with the same twin law as FeBO_3 in Fig. 3.3.6.4. Conspicuous twin element: twin reflection plane (0001), coinciding with the composition plane (0001).

3.3.6.6. Spinel twins

The twinning of rhombohedral crystals described above also occurs for cubic crystals as the *spinel law* (spinel, CaF_2 , PbS, diamond, sphalerite-type structures such as ZnS, GaAs, CdTe, cubic face- and body-centred metals). In principle, all four threefold axes of the cube, which are equivalent with respect to the *eigensymmetry* \mathcal{H} , can be active in twinning. We restrict our considerations to the case where only one threefold axis, [111], is involved. The most obvious twin operations are the twofold rotation around [111] or the reflection across (111). For centrosymmetric crystals, they are alternative twin operations and belong to the same twin law. For noncentrosymmetric crystals, however, the two operations represent different twin laws. Both cases are covered by the term ‘spinel law’.

The orientation relation defined by the spinel law corresponds to the ‘obverse’ and ‘reverse’ positions of two rhombohedra (cubes), as shown in Fig. 3.3.6.6. For the two (differently) oriented *eigensymmetries* $4/m\bar{3}2/m$ of the domain states \mathcal{H}_1 and \mathcal{H}_2 , the intersection symmetry $\mathcal{H}^* = \bar{3}2/m$ (order 12) results.

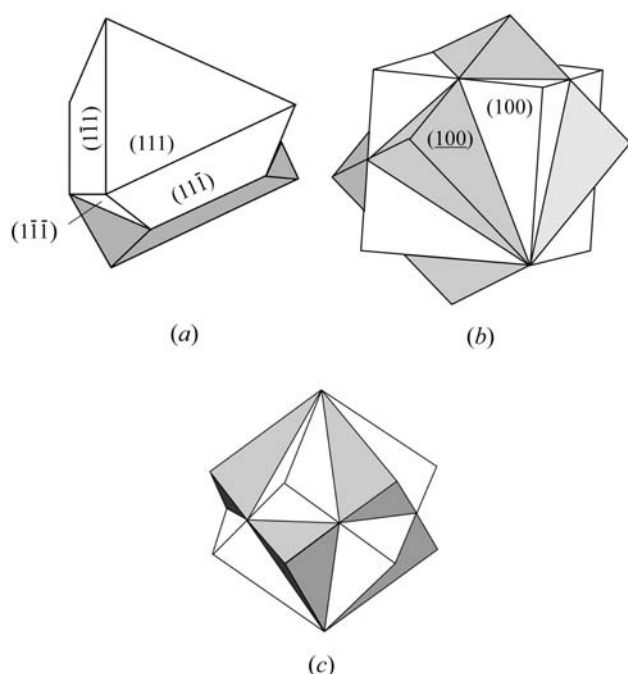


Fig. 3.3.6.6. Spinel (111) twins of cubic crystals (two orientation states). (a) Contact twin with (111) composition plane (two twin components). (b) and (c) Penetration twin (idealized) with one (111) and three {112} composition planes (twelve twin components, six of each orientation state) in two different views, (b) with one [001] axis vertical, (c) with the threefold twin axis [111] vertical.

With this ‘reduced *eigensymmetry*’ \mathcal{H}^* , the coset of 12 alternative twin operations is the same as the one derived for twinning of rhombohedral crystals in Example 3.3.6.5.

In the following, we treat the spinel twins with the twin axis [111] or the twin reflection plane (111) for the five cubic point groups (*eigensymmetries*) $\mathcal{H} = m\bar{3}m, \bar{4}3m, 432, m\bar{3}, \bar{3}2$ in detail. The intersection groups are $\mathcal{H}^* = \bar{3}2/m, 3m, 32, \bar{3}$ and 3, respectively. For these ‘reduced *eigensymmetries*’, the cosets of the alternative twin operations are listed below with reference to cubic axes.

(a) *Eigensymmetry* $\mathcal{H} = 4/m\bar{3}2/m$ (order 48), reduced *eigensymmetry* $\mathcal{H}^* = \bar{3}2/m1$ (order 12).

Alternative twin operations:

- (1) three rotations $6^1, 6^3 = 2, 6^5 = 6^{-1}$ around the axis [111];
- (2) three twofold rotations around the axes [112], [211], [121];
- (3) three reflections across the planes (112), (211), (121);
- (4) three rotoinversions around the axis [111]: $\bar{6}^1, \bar{6}^3 = m_z, \bar{6}^5 = \bar{6}^{-1}$.

Reduced composite symmetry $\mathcal{K}^* = 6'/m'(\bar{3})2/m'2'/m'$ (order 24).

(b) *Eigensymmetry* $\mathcal{H} = \bar{4}3m$ (order 24), reduced *eigensymmetry* $\mathcal{H}^* = 3m1$ (order 6).

Two different twin laws are possible:

- (1) Twin law representative: ‘twofold rotation around [111]’;
Alternative twin operations: lines (1) and (3) of case (a) above;
Reduced composite symmetry: $\mathcal{K}^* = 6'(3)mm'$ (order 12).
- (2) Twin law representative: ‘reflection across (111)’;
Alternative twin operations: lines (2) and (4) of case (a) above;
Reduced composite symmetry: $\mathcal{K}^* = 6'(3)m2' = 3/m'2m'$ (order 12).

(c) *Eigensymmetry* $\mathcal{H} = 432$ (order 24), reduced *eigensymmetry* $\mathcal{H}^* = 321$ (order 6).

Again, two different twin laws are possible:

- (1) Twin law representative: ‘twofold rotation around [111]’;
Alternative twin operations: lines (1) and (2) of case (a) above;
Reduced composite symmetry: $\mathcal{K}^* = 6'(3)22'$ (order 12).
- (2) Twin law representative: ‘reflection across (111)’;
Alternative twin operations: lines (3) and (4) of case (a) above;
Reduced composite symmetry: $\mathcal{K}^* = 6'(3)2m' = 3/m'2m'$ (order 12).

(d) *Eigensymmetry* $\mathcal{H} = 2/m\bar{3}$ (order 24), reduced *eigensymmetry* $\mathcal{H}^* = \bar{3}$ (order 6).

Two different twin laws:

- (1) Twin law representative: ‘twofold rotation around [111]’ or ‘reflection across (111)’;
Alternative twin operations: lines (1) and (4) of case (a) above;
Reduced composite symmetry: $\mathcal{K}^* = 6'/m'(\bar{3})$ (order 12).
- (2) Twin law representative: ‘reflection across (112)’ or ‘twofold rotation around [112]’;
Alternative twin operations: lines (2) and (3) of case (a) above;
Reduced composite symmetry: $\mathcal{K}^* = \bar{3}12'/m'$ (order 12).

(e) *Eigensymmetry* $\mathcal{H} = 23$ (order 12), reduced *eigensymmetry* $\mathcal{H}^* = 3$ (order 3).

Four different twin laws are possible:

- (1) Twin law representative: ‘twofold rotation around [111]’;
Alternative twin operations: line (1) of case (a) above;
Reduced composite symmetry: $\mathcal{K}^* = 6'(3)$ (order 6).
- (2) Twin law representative: ‘reflection across (111)’.
Alternative twin operations: line (4) of case (a) above.
Reduced composite symmetry: $\mathcal{K}^* = \bar{6}'(3) = 3/m'$ (order 6).
- (3) Twin law representative: ‘twofold rotation around [112]’;
Alternative twin operations: line (2) of case (a) above;
Reduced composite symmetry $\mathcal{K}^* = 312'$ (order 6).

3. PHASE TRANSITIONS, TWINNING AND DOMAIN STRUCTURES

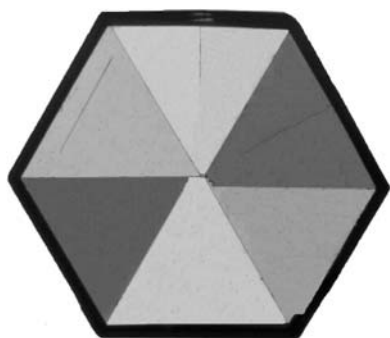


Fig. 3.3.6.7. Pseudo-hexagonal growth twin of K_2SO_4 showing six sector domains in three orientation states. (001) plate, about 1 mm thick and 5 mm in diameter, between polarizers deviating by 45° from crossed position for optimal contrast of all domains. The crystal was precipitated from aqueous K_2SO_4 solution containing 5% S_2O_3 ions. Courtesy of M. Moret, Milano.

- (4) Twin law representative: 'reflection across $(11\bar{2})'$;
 Alternative twin operations: line (3) of case (a) above;
 Reduced composite symmetry: $\mathcal{K}^* = 31m'$ (order 6).

The restriction to only one of the four spinel twin axes $\langle 111 \rangle$ combined with the application of the coset expansion to the *reduced eigensymmetry* \mathcal{H}^* always leads to a crystallographic composite symmetry \mathcal{K}^* . The supergroup generated from the *full eigensymmetry*, however, would automatically include the other three spinel twin axes and thus would lead to the infinite sphere group $m\bar{3}c$, *i.e.* would imply infinitely many cosets and (equivalent) twin laws. Higher-order spinel twins are discussed in Section 3.3.8.3.

3.3.6.7. Growth and transformation twins of K_2SO_4

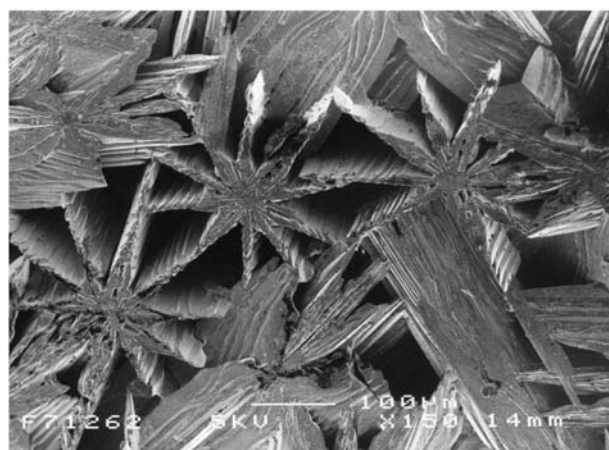
K_2SO_4 has an orthorhombic pseudo-hexagonal room-temperature phase with point group $\mathcal{H} = mmm$ and axial ratio $b/a = \tan 60.18^\circ$, and a hexagonal high-temperature phase (> 853 K) with supergroup $\mathcal{G} = 6/m2/m2/m$. It develops pseudo-hexagonal growth-sector twins with equivalent twin reflection planes (110) and $(\bar{1}\bar{1}0)$ which are also composition planes, as shown in Fig. 3.3.6.7. As discussed in Sections 3.3.2.3.2 and 3.3.4.4 under (iii), this corresponds to a pseudo-threefold twin axis which, in combination with the twofold *eigensymmetry* axis, is also a pseudo-hexagonal twin axis. The extended composite symmetry is

$$\mathcal{K}(6) = \mathcal{K}(3) = 6(2)/m2/m2/m.$$

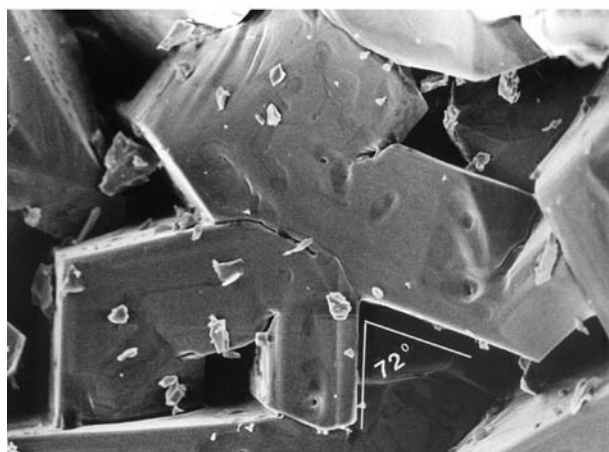
Upon heating above 853 K, the growth-sector twinning disappears. On cooling back into the low-temperature phase, transformation twinning ('domain structure') with three systems of lamellar domains appears. The three orientation states are identical for growth and transformation twins, but the morphology of the twins is not: sectors *versus* lamellae. The composite symmetry \mathcal{K} of the twins at room temperature is the true structural symmetry \mathcal{G} of the 'parent' phase at high temperatures.

3.3.6.8. Pentagonal–decagonal twins

As was pointed out in Note (8) of Section 3.3.2.4 and in part (iii) of Section 3.3.4.4, there exist twin axes with noncrystallographic multiplicities $n = 5, 7, 8$ etc. Twins with five- or tenfold rotations are frequent in intermetallic compounds. As an example, $FeAl_4$ is treated here (Ellner & Burkhardt, 1993; Ellner, 1995). This compound is orthorhombic, $2/m2/m2/m$, with an axial ratio close to $c/a = \tan 72^\circ$, corresponding to a pseudo-fivefold axis along $[010]$ and equivalent twin mirror planes (101) and $(\bar{1}01)$, which are about 36° apart. In an ideal intergrowth, this leads to a cyclic pseudo-pentagonal or pseudo-decagonal sector



(a)



(b)

Fig. 3.3.6.8. Pentagonal–decagonal twins. (a) Decagonal twins in the shape of tenfold stars on the surface of a bulk alloy, formed during the solidification of a melt of composition $Ru_8Ni_{15}Al_{77}$. Scanning electron microscopy picture. Typical diameter of stars *ca.* 200 μm . The arms of the stars show parallel intergrowth. (b) Pentagonal twin aggregate of Fe_4Al_{13} with morphology as grown in the orthorhombic high-temperature phase, showing several typical 72° angles between neighbouring twin partners (diameter of aggregate *ca.* 200 μm). Orthorhombic lattice parameters $a = 7.7510$, $b = 4.0336$, $c = 23.771$ \AA , space group $Bmmm$. The parameters c and a approximate the relation $c/a = \tan 72^\circ$; the pseudo-pentagonal twin axis is $[010]$. On cooling, the monoclinic low-temperature phase is obtained. The twin reflection planes in the orthorhombic unit cell are (101) and $(\bar{1}01)$, in the monoclinic unit cell (100) and (201) ; cf. Ellner & Burkhardt (1993, Fig. 10), Ellner (1995). Both parts courtesy of M. Ellner, Stuttgart.

twin (Fig. 3.3.6.8). All features of this twinning are analogous to those of pseudo-hexagonal aragonite, treated in Section 3.3.2.3.2, and of K_2SO_4 , described above as Example 3.3.6.7.

The intersection symmetry of all twin partners is $\mathcal{H}^* = 12/m1$; the reduced composite symmetry \mathcal{K}^* of a domain pair in contact is $2'/m2/m2'/m$. The extended composite symmetry of the ideal pentagonal sector twin is $\mathcal{K}(10) = \mathcal{K}(5) = 10(2)/m2/m2/m$.

3.3.6.9. Multiple twins of rutile

Rutile with *eigensymmetry* $4/m2/m2/m$ develops growth twins with coinciding twin reflection and composition plane $\{011\}$. Owing to its axial ratio $a/c = \tan 57.2^\circ$, the tetragonal c axes of the two twin partners form an angle of 114.4° . The intersection symmetry of the two domains is $\mathcal{H}^* = 2/m$ along the common direction $[100]$. The reduced composite symmetry of the domain pair is $\mathcal{K}^* = 2/m2'/m'2'/m'$, with the primed twin elements parallel and normal to the plane (011) . A twin of this type, consisting of two domains, is called an 'elbow twin' or a 'knee twin', and is shown in Fig. 3.3.6.9(a).

3.3. TWINNING OF CRYSTALS

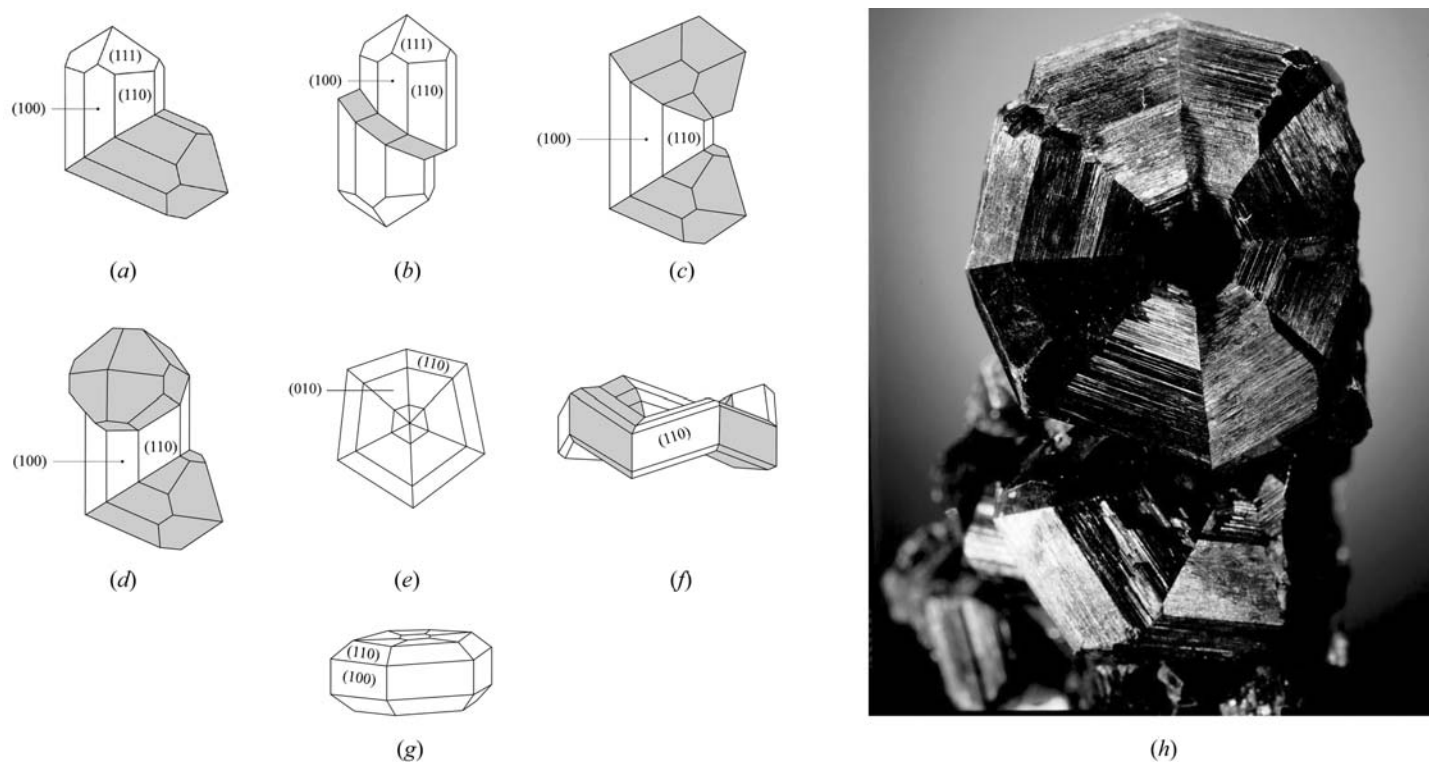


Fig. 3.3.6.9. Various forms of rutile (TiO_2) twins, with one or several equivalent twin reflection planes $\{011\}$. (a) Elbow twin (two orientation states). (b) Twin with two orientation states. One component has the form of an inserted lamella. (c) Triple twin (three orientation states) with twin reflection planes (011) and $(0\bar{1}1)$. (d) Triple twin with twin reflection planes (011) and (101) . (e) Cyclic sixfold twin with six orientation states. Two sectors appear strongly distorted due to the large angular excess of 35.6° . (f) Cyclic eightfold twin with eight orientation states. (g) Perspective view of the cyclic twin of (e). (h) Photograph of a rutile eightling (ca. 15 mm diameter) from Magnet Cove, Arkansas (Geologisk Museum, Kopenhagen). Parts (a) to (e) courtesy of H. Strunz, Unterwössen, cf. Ramdohr & Strunz, 1967, p. 512. Photograph (h) courtesy of M. Medenbach, Bochum.

In point group $4/m2/m2/m$, there exist four equivalent twin reflection planes $\{011\}$ (four different twin laws) with angles of 65.6° between (001) and $(0\bar{1}1)$ and 45° between (011) and (101) , leading to a variety of multiple twins. They may be linear polysynthetic or multiple elbow twins, or any combination thereof (Fig. 3.3.6.9). Very rare are complete cyclic sixfold twins with a large angular excess of $6 \times 5.6^\circ = 33.6^\circ$ (corresponding formally to a '5.5-fold' twin axis) and extended composite pseudosymmetry $\mathcal{K}(6) = 6(2)/m2/m2/m$, or cyclic eightfold twins with a nearly exact fit of the sectors and a morphological pseudo-8 twin axis. In the 'sixling', the tetragonal axes of the twin components are coplanar, whereas in the 'eightling' they alternate 'up and down', exhibiting in ideal development the morphological symmetry $82m$ of the twin aggregate. The extended composite symmetry is $\mathcal{K}(8) = 8(1)/m2/m2/m$ with eight twin components, each of different orientation state. These cyclic twins are depicted in Figs. 3.3.6.9(e), (f), (g) and (h).

The sketch of the 'eightling' in Fig. 3.3.6.9(f) suggests a hole in the centre of the ring, a fact which would pose great problems for the interpretation of the origin of the twin: how do the members of the ring 'know' when to turn and close the ring without an offset? Fig. 3.3.6.9(h) suggests that the ring is covered at the back, i.e. originates from a common point (nucleus). This was confirmed by a special investigation of another 'eightling' from Magnet Cove (Arkansas) by Lieber (2002): the 'eightling' started to grow from the nucleus and developed into the shape of a funnel with an opening of increasing diameter in the centre. This proves the nucleation growth of the ring (cf. Section 3.3.7.1.1).

3.3.6.10. Variety of twinning in gibbsite, $\text{Al}(\text{OH})_3$

Gibbsite (older name: hydrargillite) forms a pronounced layer structure with a perfect cleavage plane (001) . It is monoclinic with eigensymmetry $\mathcal{H} = 12/m1$, but strongly pseudo-hexagonal with

an axial ratio $b/a = \tan 30.4^\circ$. In contrast to most other pseudo-hexagonal crystals, the twofold eigensymmetry axis b is not parallel but normal to the pseudo-hexagonal c axis. The normal to the cleavage plane (001) is inclined by $\beta - 90^\circ = 4.5^\circ$ against $[001]$. Owing to the pseudo-hexagonal metrics of the plane (001) , the lattice planes (110) and $(\bar{1}10)$, equivalent with respect to the eigensymmetry $\mathcal{H} = 2/m$, form an angle of 60.8° .

The following four significant twin laws have been observed by Brögger (1890):

(i) *(001) reflection twin*: the cleavage plane (001) acts both as twin mirror and composition plane. The pseudo-hexagonal axes $[001]$ of both partners are inclined to each other by 9.0° . This twin law is quite common in natural and synthetic gibbsite.

(ii) *(100) reflection twin*: the twin mirror plane (100) is also the composition plane. The angle between the (001) planes of both partners is 9.0° , as in (i); the pseudo-hexagonal axes $[001]$ of both partners are parallel. This twin law is not common.

(iii) *(110) reflection twin*: again, twin mirror plane and composition plane coincide. The two (001) planes span an angle of 4.6° . This twin law is very rare in nature, but is often observed in synthetic materials. A sixfold sector twin of synthetic gibbsite, formed by cyclic repetition of $\{110\}$ twin reflection planes 60.8° apart, is shown in Fig. 3.3.6.10. The pseudo-hexagonal axis $[001]$ is common to all domains. Since the (001) plane is inclined towards this axis at 94.5° , the six (001) facets of the twinned crystal form a kind of 'umbrella' with $[001]$ as umbrella axis (Fig. 3.3.6.10a). This (001) umbrella faceting was recently observed in twinned synthetic gibbsite crystals by Sweegers *et al.* (1999).

In contrast to orthorhombic aragonite with only three pseudo-hexagonal orientation states, these gibbsite twins exhibit six different orientation states. This is due to the absence of any eigensymmetry element along the pseudo-hexagonal axis $[001]$. The intersection symmetry of all orientation states is 1. The reduced composite symmetry of a domain pair is $\mathcal{K}^* = 12'/m'1$, with m' the twin mirror plane (110) .

3. PHASE TRANSITIONS, TWINNING AND DOMAIN STRUCTURES

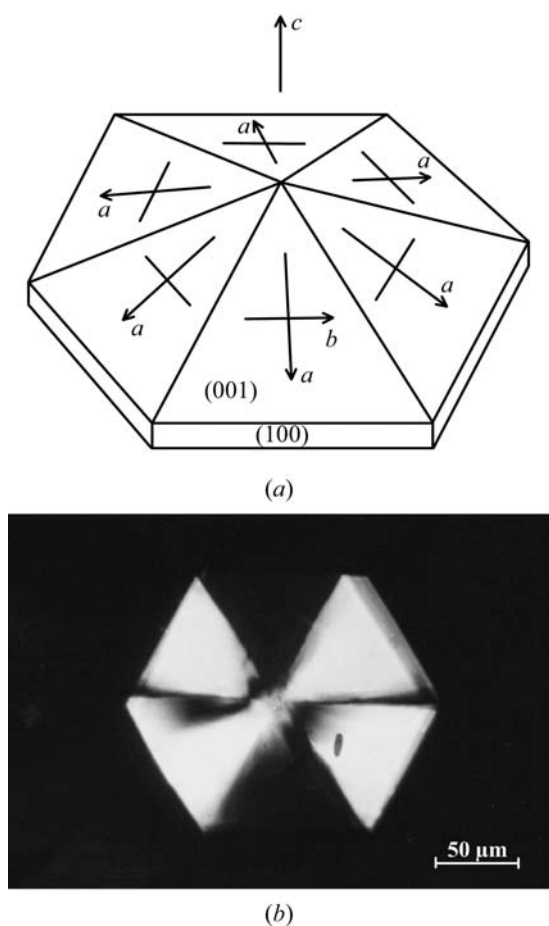


Fig. 3.3.6.10. Sixfold reflection twin of gibbsite, $\text{Al}(\text{OH})_3$, with equivalent (110) and $(\bar{1}\bar{1}0)$, both as twin mirror and composition planes. (a) Perspective view of a tabular sixfold sector twin with pseudo-hexagonal twin axis c . In each sector the monoclinic b axis is normal to the twin axis c , whereas the a axis slopes slightly down by about 4.5° ($\beta = 94.5^\circ$), leading to an umbrella-like shape of the twin. (b) Polarization micrograph of a sixfold twinned hexagon (six orientation states) of the shape shown in (a). Pairs of opposite twin components have the same optical extinction position. Courtesy of Ch. Sweegers, PhD thesis, University of Nijmegen, 2001.

(iv) ‘Median law’: According to Brögger (1890), this twin law implies exact parallelism of non-equivalent edges $[110]_{\text{I}}$ and $[010]_{\text{II}}$, and *vice versa*, of partners I and II. The twin element is an irrational twofold axis parallel to (001) , bisecting *exactly* the angle between $[110]$ and $[010]$, or alternatively, an irrational twin reflection plane normal to this axis. This interesting orientation relation, which has been observed so far only for gibbsite, does not obey the minimum condition for twinning as set out in Section 3.3.2.2. An alternative interpretation, treating these twins as *rational* $[130]$ rotation twins, is given by Johnsen (1907), *cf.* Tertsch (1936), pp. 483–484. Interestingly, this strange ‘twin law’ is the most abundant one among natural gibbsite twins.

3.3.6.11. Plagioclase twins

From the point of view of the relationship between pseudosymmetry and twinning, triclinic crystals are of particular interest. Classical mineralogical examples are the plagioclase feldspars with the ‘albite’ and ‘pericline’ twin laws of triclinic (crystal class $\bar{1}$) albite $\text{NaAlSi}_3\text{O}_8$ and anorthite $\text{CaAl}_2\text{Si}_2\text{O}_8$ (also microcline, triclinic KAlSi_3O_8), which all exhibit strong pseudosymmetries to the monoclinic feldspar structure of sanidine. Microcline undergoes a very sluggish monoclinic–triclinic phase transformation involving Si/Al ordering from sanidine to microcline, whereas albite experiences a quick, displacive transformation from monoclinic monalbite to triclinic albite.

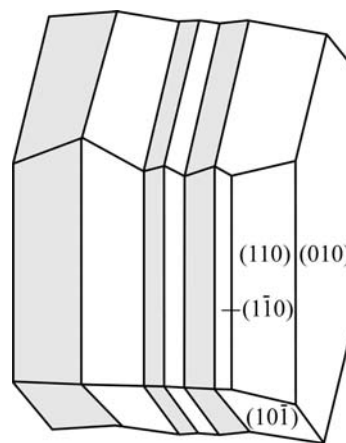


Fig. 3.3.6.11. Polysynthetic albite twin aggregate of triclinic feldspar, twin reflection and composition plane (010) .

The composite symmetries of these twins can be formulated as follows:

Albite law: reflection twin on (010) ; composition plane (010) rational (Fig. 3.3.6.11, Table 3.3.6.5). $\mathcal{K}_A = 2'/m'(\bar{1})$ with rational $m' \parallel (010)$.

Pericline law: twofold rotation twin along $[010]$; composition plane irrational $\parallel [010]$: ‘rhombic section’ (Fig. 3.3.6.12, Table 3.3.6.5). $\mathcal{K}_P = 2'/m'(\bar{1})$ with rational $2' \parallel [010]$.

Both twin laws resemble closely the monoclinic pseudosymmetry $2/m$ in two slightly different but distinct fashions: each twin law \mathcal{K} uses one rational twin element from $2/m$, the other one is irrational. The two frameworks of twin symmetry $2'/m'$ are inclined with respect to each other by about 4° , corresponding to the angle between b (direct lattice) and b^* (reciprocal lattice).

Both twins occur as growth and transformation twins: they appear together in the characteristic lamellar ‘transformation microclines’.

3.3.6.12. Staurolite

The mineral staurolite, approximate formula $\text{Fe}_2\text{Al}_9[\text{O}_6(\text{O},\text{OH})_2(\text{SiO}_4)_4]$, has ‘remained an enigma’ (Smith, 1968) to date with respect to the subtle details of symmetry, twinning, structure and chemical composition. A lively account of these problems is provided by Donnay & Donnay (1983). Staurolite is strongly pseudo-orthorhombic, C_{2mm} , and only detailed optical, morphological and X-ray experiments reveal monoclinic symmetry, $C_{12/m1}$, with $a = 7.87$, $b = 16.62$, $c = 5.65 \text{ \AA}$ and $\beta = 90^\circ$ within experimental errors (Hurst *et al.*, 1956; Smith, 1968).

Staurolite exhibits two quite different kinds of twins:

(i) *Twinning by high-order merohedry* (after Friedel, 1926, p. 56) was predicted by Hurst *et al.* (1956) in their detailed study of staurolite twinning. Staurolite crystals are supposed to consist of very fine scale monoclinic ($\mathcal{H} = 12/m1$) microtwins on $m(001)$, which yield a twin aggregate of orthorhombic composite symmetry $\mathcal{K} = 2'/m'2/m2'/m'$. The coset consists of $m'(001)$, $m'(100)$, $2' \parallel [100]$ and $2' \parallel [001]$. Even though this twinning appears highly probable due to the pronounced structural pseudosymmetry (‘high-order merohedry’) of staurolite and has been mentioned by several authors (*e.g.* Smith, 1968), so far it has never been unambiguously proven. In particular, electron-microscopy investigations by Fitzpatrick (1976, quoted in

Table 3.3.6.5. Plagioclase: albite and pericline twins

\mathcal{H}	$k \times \mathcal{H}$ (albite)	$k \times \mathcal{H}$ (pericline)
1	$m \parallel (010)$ rational	$2 \parallel [010]$ rational
$\bar{1}$	$2 \perp (010)$ irrational	$m \perp [010]$ irrational

3.3. TWINNING OF CRYSTALS

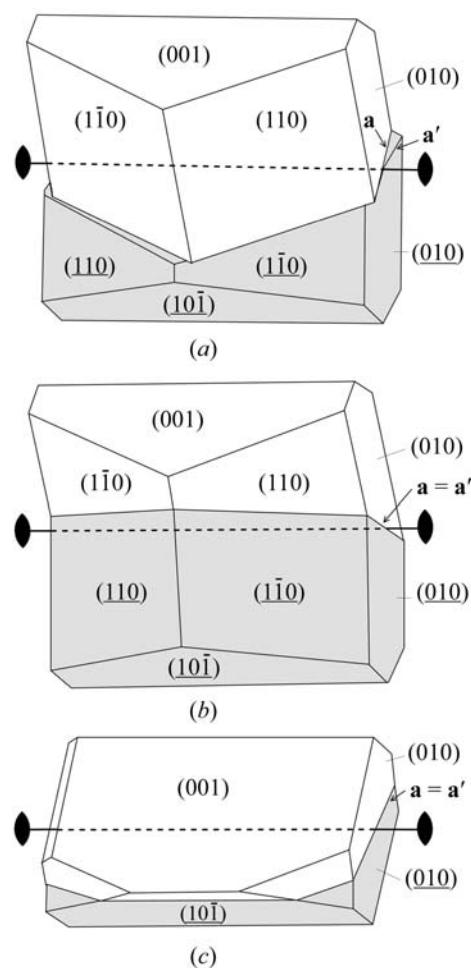


Fig. 3.3.6.12. Pericline twin of triclinic feldspar. Twofold twin axis $[010]$. (a) Twin with rational composition plane (001) , exhibiting clearly the misfit (exaggerated) of the two adjacent (001) contact planes, as indicated by the crossing of lines **a** and **a'**. (b) The same (exaggerated) twin as in (a) but with irrational boundary along the 'rhombic section': fitting of contact planes from both sides (**a** and **a'** coincide and form a flat ridge). (c) Sketch of a real pericline twin with irrational interface ('rhombic section') containing the twin axis.

Bringhurst & Griffin, 1986, p. 1470) have failed to detect the submicroscopic twins.

(ii) Superimposed upon this first generation of microtwins very often occurs one or the other of two spectacular 'macroscopic' growth penetration twins in the shape of a cross, from which in 1792 the name 'stauros' of the mineral was given by Delam  theri  . The first detailed analysis of these twins was provided by Friedel (1926, p. 461).

(a) The 90° cross (Greek cross) with twin reflection and composition plane (031) is illustrated in Fig. 3.3.6.13(a) [cf. also the figures on p. 151 of Hurst *et al.* (1956) for less idealized drawings]. Plane (031) generates two twin components with an angle of $2 \arctan(b/3c) = 2 \arctan 0.9805 = 88.9^\circ$, very close to 90° , between their c axes. The equivalent twin reflection plane $(0\bar{3}1)$ leads to the same angle, and both twin planes intersect along the lattice row $[100]$.

With eigensymmetry $\mathcal{H} = 12/m1$, the intersection symmetry of the domain pair is $\mathcal{H}^* = 1$ and the reduced composite symmetry is $\mathcal{K}^* = 2'/m'$ [$m' = (031)$]. Owing to the special axial ratio $b/3c \approx 1$ mentioned above, the 90° cross is an excellent example of a pseudo-tetragonal twin. The extended composite symmetry of this twin is oriented along $[100]$:

$$\mathcal{K}(4) = 4(2)/m2/m2/m$$

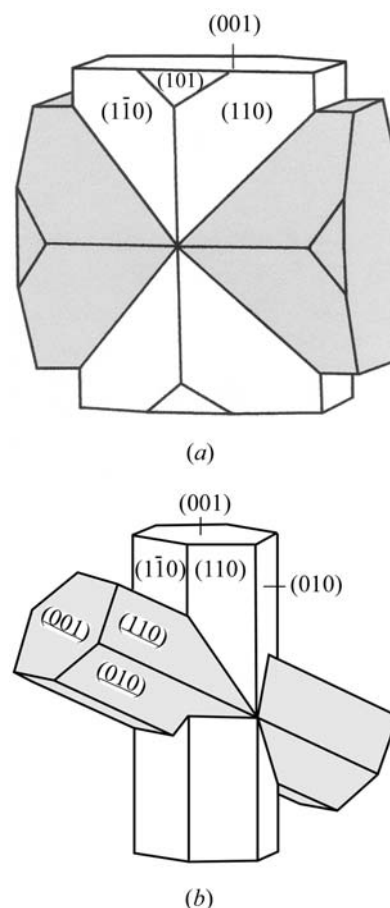


Fig. 3.3.6.13. Twinning of staurolite. (a) 90° cross ('Greek cross') with twin reflection and composition planes (031) and (031) . (b) 60° cross ('St Andrew's cross') with twin reflection and composition plane (231) .

[cf. Section 3.3.4.2(iii)] with two domain states and all twin operations binary.

(b) The 60° cross (St Andrew's cross) with twin reflection plane (231) is illustrated in Fig. 3.3.6.13(b). It is the more abundant of the two crosses, with a ratio of $60^\circ : 90^\circ$ twins $\approx 9 : 1$ in one Georgia, USA, locality (cf. Hurst *et al.*, 1956, p. 152). Two equivalent twin mirror planes, (231) and $(\bar{2}\bar{3}1)$, intersecting in lattice row $[102]$ exist. They include an angle of 60.4° . The action of one of these twin reflection planes leads to the 60° cross with an angle of 60° between the two c axes. The reduced composite symmetry of this twin pair is $\mathcal{K}^* = 2'/m'$ [$m' = (231)$].

In rare cases, penetration trillings occur by the action of both equivalent mirror planes, (231) and $(\bar{2}\bar{3}1)$, leading to three interpenetrating twin components with angles of about 60° between neighbouring arms.

Notes

(1) In many books, the twin reflection planes for the 90° cross and the 60° cross are given as (032) and (232) instead of (031) and (231) . The former Miller indices refer to the morphological cell, which has a double c axis compared with the structural X-ray cell, used here.

(2) Friedel (1926) and Hurst *et al.* (1956) have derived both twin laws (031) and (231) , mentioned above, from a multiple cubic pseudo-cell, the 'Mallard pseudo-cube'. This derivation will be presented in Section 3.3.9.2.4 as a characteristic example of 'twinning by reticular pseudo-merohedry'.

3.3.6.13. $BaTiO_3$ transformation twins

The perovskite family, represented by its well known member $BaTiO_3$, is one of the technically most important groups of dielectric materials, characterized by polar structures which

3. PHASE TRANSITIONS, TWINNING AND DOMAIN STRUCTURES

exhibit piezoelectricity, pyroelectricity and, most of all, ferroelectricity.

BaTiO₃ is cubic and centrosymmetric (paraelectric) above 393 K. Upon cooling below this temperature it transforms in one step (first-order transformation with small ΔH) into the ferroelectric tetragonal phase with polar space group $P4mm$. This transition is *translationengleich* of index $[i] = 6$. Hence there are domains of six possible orientation states at room temperature. The transformation can be theoretically divided into two steps:

(i) *Translationengleiche* symmetry reduction cubic $Pm\bar{3}m \rightarrow$ tetragonal $P4/mmm$ of index $[i_1] = 3$, leading to three sets of *ferroelastic* '90° domains', related by the (lost) cubic {110} twin mirror planes or the (lost) cubic threefold axes. These three pseudo-merohedral orientation states point with their tetragonal c axes along the three former cube axes [100], [010] and [001], thus including angles of nearly 90°.

(ii) Each of these centrosymmetric domains splits into two *antiparallel* polar ferroelectric '180° domains', whereby the space group $P4/mmm$ is *translationsgleich* reduced to $P4mm$ of index $[i_2] = 2$. The total index is: $[i] = [i_1] \cdot [i_2] = 6$.

The beautiful polysynthetic twin structure of BaTiO₃ is shown in the colour micrograph Fig. 3.4.1.1 in Chapter 3.4 of this volume.

3.3.6.14. Twins of twins

This term is due to Henke (2003) and refers to the simultaneous occurrence (superposition) of two or more different twin types (twin laws) in one and the same crystal. In *twins of twins*, one 'generation' of twin domains is superimposed upon the other, each with its own twin law. This may occur as a result of:

- (1) two successive phase transitions, each with its own twinning scheme, or
- (2) one phase transition with loss of two kinds of symmetry elements, or
- (3) a phase transition superimposed on an existing growth twin.

Typical examples are:

(i) the cubic–tetragonal ($m\bar{3}m \rightleftharpoons 4mm$) phase transition of BaTiO₃, described above. Here, 90° domains (due to the loss of the diagonal mirror planes) are superimposed by 180° domains (due to the loss of the inversion centres);

(ii) a similar case (tetragonal–monoclinic) is provided by the 'type case' of Henke (2003), (NO)₂VCl₆;

(iii) ammonium lithium sulfate exhibits pseudo-hexagonal growth-sector twins upon which lamellae of ferroelectric 180° domains are superimposed.

In this context, the term *complete twin* should be noted. It was coined by Curien & Donnay (1959) for the symmetry description of a crystal containing several merohedral twin laws. Their preferred example was quartz, but there are many relevant cases:

(i) The complete merohedral 'twins of twins' of quartz, *i.e.* the superposition of the Dauphiné, Brazil and Leydolt twins, can be formulated as follows:

Dauphiné twin law: $321 \Rightarrow 6'(3)22'$

Brazil twin law: $321 \Rightarrow \bar{3}'(3)2/m'1(\bar{1}')$

Leydolt twin law: $321 \Rightarrow \bar{6}'(3)2m' = 3/m'2m'$.

Combination = 'complete twin': $6'(3)/m'2/m'2'/m'(\bar{1}')$; this symmetry corresponds to the hexagonal holohedral point group $6/m2/m2/m$, *cf.* Example 3.3.6.3.

(ii) Another example is provided by KLiSO₄ (crystal class 6), extensively investigated by Klapper *et al.* (1987):

Inversion twins: $6 \Rightarrow 6/m'(\bar{1}')$

Reflection twins: $6 \Rightarrow 6m'm'$

Rotation twins: $6 \Rightarrow 62'2'$.

Combination = 'complete twin': $6/m'2'/m'2'/m'(\bar{1}')$; this symmetry is isomorphic to the complete-twin symmetry of quartz, given above, and to the hexagonal holohedral point group $6/m2/m2/m$.

3.3.7. Genetic classification of twins

In Section 3.3.3, a classification of twins based on their morphological appearance was given. In the present section, twins are classified according to their origin. Genetic terms such as growth twins, transformation twins and mechanical twins were introduced by Buerger (1945) and are in widespread use. They refer to the *physical origin* of a given twin in contrast to its geometrical description in terms of a twin law. The latter can be the same for twins of different origin, but it will be seen that the generation of a twin has a strong influence on the shape and distribution of the twin domains. An extensive survey of the genesis of all possible twins is given by Cahn (1954).

3.3.7.1. Growth twinning

Growth twins can occur in nature (minerals), in technical processes or in the laboratory during growth from vapour, melt or solution. Two mechanisms of generation are possible for growth twins:

- (i) formation during nucleation of the crystal;
- (ii) formation during crystal growth.

3.3.7.1.1. Twinning by nucleation

In many cases, twins are formed during the first stages of spontaneous nucleation, possibly before the sub-critical nucleus reaches the critical size necessary for stable growth. This idea was originally proposed by Buerger (1945, p. 476) under the name *supersaturation twins*. There is strong evidence for twin formation during nucleation for penetration and sector twins, where all domains originate from one common well defined 'point' in the centre of the twinned crystal, which marks the location of the spontaneous nucleus.

Typical examples are the *penetration twins* of iron borate FeBO₃ (calcite structure), which are intergrowths of two rhombohedra, a reverse and an obverse one, and consist of 12 alternating twin domains belonging to two orientation states (see Example 3.3.6.5 and Fig. 3.3.6.4). Experimental details are presented by Klapper (1987) and Kotrbova *et al.* (1985). Further examples are the penetration twins of the spinel law (Example 3.3.6.6 and Fig. 3.3.6.6), the very interesting and complex [001] penetration twin of the monoclinic feldspar orthoclase (Fig. 3.3.7.1) and the *sector twins* of ammonium lithium sulfate with three orientation states (Fig. 3.3.7.2).

It should be emphasized that *all* iron borate crystals that are nucleated from flux or from vapour (chemical transport) exhibit penetration twinning. The occurrence of untwinned crystals has not been observed so far. Crystals of isostructural calcite and NaNO₃, on the other hand, do not exhibit penetration twins at all. In contrast, for ammonium lithium sulfate, NH₄LiSO₄, both sector-twinned and untwinned crystals occur in the same batch. In this case, the frequency of twin formation increases with higher supersaturation of the aqueous solution.

The formation of *contact twins* (such as the dovetail twins of gypsum) during nucleation also occurs frequently. This origin must always be assumed if both partners of the final twin have roughly the same size or if all spontaneously nucleated crystals in one batch are twinned. For example, all crystals of monoclinic